AIP | Applied Physics Letters

Magnetoelastic coupling induced magnetic anisotropy in Co2(Fe/Mn)Si thin films

Himanshu Pandey, P. K. Rout, Anupam, P. C. Joshi, Z. Hossain, and R. C. Budhani

Citation: Applied Physics Letters **104**, 022402 (2014); doi: 10.1063/1.4861777
View online: http://dx.doi.org/10.1063/1.4861777
View Table of Contents: http://scitation.aip.org/content/aip/journal/apl/104/2?ver=pdfcov
Published by the AIP Publishing

Magnetoelastic coupling induced magnetic anisotropy in Co_2(Fe/Mn)Si thin films

Himanshu Pandey,[1] P. K. Rout,[1] Anupam,[1] P. C. Joshi,[1] Z. Hossain,[1] and R. C. Budhani[1,2,a)]
[1]*Condensed Matter-Low Dimensional Systems Laboratory, Department of Physics, Indian Institute of Technology Kanpur, Kanpur 208016, India*
[2]*CSIR-National Physical Laboratory, New Delhi 110012, India*

(Received 30 October 2013; accepted 28 December 2013; published online 13 January 2014)

We report the influence of in-plane strain on uniaxial magnetic anisotropy of Co_2(Fe/Mn)Si [CF(M)S] films grown on $SrTiO_3$ (STO) and MgO by varying film thickness. The analysis of magnetic free energy functional for the films on STO showed the presence of magnetoelastic anisotropy with magnetostriction constant of 12.22×10^{-6} for CFS and 2.02×10^{-6} for CMS in addition to intrinsic magnetocrystalline anisotropy. Single-domain phase diagram reveals a gradual transition from in-plane to canted state with decreasing film thickness due to strain-induced tetragonal distortion. A maximum canting angle of 41.5° with respect to film plane is predicted for CFS (12 nm)/STO film. © *2014 AIP Publishing LLC*. [http://dx.doi.org/10.1063/1.4861777]

The Heusler alloys have taken the center stage as spintronics materials due to their high degree of spin polarization, high Curie temperature, and low magnetic damping.[1,2] By tuning the magnetic parameters such as coercivity, anisotropy, exchange interactions, and damping processes, one can suitably tailor these materials for magnetic random access memory, magnetic logics, spin-transistors, and related potential applications. However, in most of such applications the magnetic alloy has to be in a thin film form in which its magnetic characteristics can be significantly different due to film thickness, crystallographic orientation, growth related strains, and interfacial reactions. One such characteristics is magnetic anisotropy, which should be large for magnetic storage applications, and which also determines the magnetization reversal processes in magnetic switching devices. Till now, a large number of full-Heusler alloy thin films have been grown on various substrates. Some examples of this are Co_2MnGe on GaAs (Ref. 3) and Al_2O_3,[4] Co_2MnSi on GaAs,[5] MgO,[6–8] and Al_2O_3,[9] $Co_2FeAl_{0.5}Si_{0.5}$ on MgO,[10] Co_2FeSi on GaAs,[11,12] Al_2O_3,[13] and MgO (Ref. 13) as well as on $SrTiO_3$ (STO).[14–16] While the substrate lattice parameter, growth, thermal annealing condition, and film thickness in these cases vary significantly, the effect of such condition on magnetic anisotropy of the films is seldom addressed. In Heusler alloys films, one expects a four-fold anisotropy due to the cubic symmetry of the unit cell, while in-plane uniaxial anisotropy has also been observed for the case of Co_2FeSi grown on GaAs.[11] The presence of additional uniaxial anisotropy has resulted in multistep magnetization switching in some Heusler alloy films.[3,5] Moreover, Gabor *et al*. have shown that Co_2FeAl films can have three types of in-plane anisotropies, namely, biaxial (fourfold cubic anisotropy) and two uniaxial anisotropies parallel to the biaxial easy and hard axes.[17] In some cases, stripe domains have also been seen due to magnetic frustration between two energetically equivalent easy axis.[18] The interface between the film and substrate also affects the orientation of magnetization significantly. For example, the out-of-plane magnetic easy axis in Co_2FeAl films on Cr-buffered MgO substrate seemed to be induced by the interfacial anisotropy, which appears after annealing the films in the presence of magnetic field applied along out-of-plane direction.[19]

The magnetic anisotropy in thin films originates from fundamental factors such as the spin-orbit interaction in the material which controls magnetocrystalline anisotropy and/or due to growth related strain. Any change in the lattice via strain will change the distances between the magnetic atoms and alter the interaction energy, which decides the magnetoelastic anisotropy.[20] The strain therefore becomes a tuning parameter for magnetic anisotropy and can be varied by a choice of substrates with different lattice parameters or by varying the film thickness. A consequence of the strain related anisotropy is the rotation of magnetic easy axes from in-plane to out-of-plane configuration or vice versa.[21–24] While the strain dependence of in-plane anisotropy has been reported for Co_2FeAl/MgO thin films,[17] the strain driven out-of-plane anisotropy in Heusler alloy films requires more attention.

Here, we report a detailed study of the magnetic anisotropy in Co_2(Fe/Mn)Si [CF(M)S] films of various thickness deposited on (001) MgO and (001) STO crystals. The in-plane biaxial strain was gradually varied from compressive (for the films on STO) to tensile (for the films on MgO) by depositing the films of different thickness. We have specifically focused on the strain dependence of out-of-plane uniaxial magnetic anisotropy in CF(M)S/STO films and established how the strain induced magnetic anisotropy affects the direction of magnetization. It is seen that the tuning of magnetoelastic coupling by varying the film thickness results in the rotation of the magnetization vector towards out-of-plane direction as the film thickness is lowered in case of the films on STO.

We have previously demonstrated that the CF(M)S films on STO and MgO processed at 600 °C have better crystalline quality as compared to those annealed at lower temperatures.[6,7,14] Therefore, for studies of anisotropy reported here, we mainly concentrate on the films processed at 600 °C. The cubic lattice parameter $(a_{bulk} \approx 0.5656\,\text{nm})$ of CF(M)S matches quite well with the face diagonal $(\sqrt{2}a_{sub})$ of (001)

a)Electronic addresses: rcb@iitk.ac.in and rcb@nplindia.org

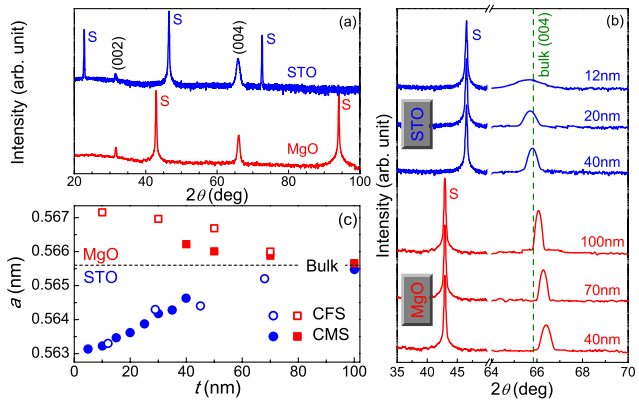

FIG. 1. (a) The $\theta - 2\theta$ X-ray diffraction profiles of 40 nm thick CMS films grown on STO and MgO. (b) The $\theta - 2\theta$ scans about (004) peak of CMS films on STO and MgO with different thicknesses. The Bragg reflections from (002) planes of the substrates are marked as "S". The dashed line shows the position of 2θ value corresponding to (004) peak of bulk CMS. (c) The in-plane (a) lattice parameter as a function of film thickness t for CMS (filled symbols) and CFS (empty symbols). The cubic lattice parameter of bulk CF(M)S is marked by the dotted line.

STO and MgO. The lattice misfit $[\epsilon = (a - \sqrt{2}a_{sub})/\sqrt{2}a_{sub}]$ of CF(M)S with STO and MgO lies within 6%. Taking advantage of close matching of the lattice parameters, we have prepared a series of CF(M)S thin films of various thickness ($t = 5$-100 nm) epitaxially on (001) STO and MgO using pulsed laser deposition technique. The details of thin film preparation are described in our earlier reports.[6,7,14,15] The structural characterization of the films has been performed by X-ray diffraction (PANalytical X'Pert PRO X-ray diffractometer) in θ-2θ, ω, φ, and grazing incidence X-ray diffraction modes. The magnetic measurements were performed in a vibrating sample magnetometer (EV7 VSM) at room temperature.

The $\theta - 2\theta$ X-ray diffraction reveals (00l) oriented growth of CF(M)S films on STO and MgO [Fig. 1(a)]. Further evidence of (00l) texturing is provided by the rocking curves about (004) reflection. The full width at half maximum of these films are less than 1.9°, which corresponds to a crystallite size of 5 nm.[15] Moreover, the φ scans confirm the epitaxial growth of the films with the relation [100] CF(M)S ‖ [110] STO or MgO. The presence of (111) superlattice, which governs the ordering of the Fe (or Mn) and Si sublattices, and (022) fundamental diffraction line, which confirms the presence of $L2_1$ ordering in the films, are two important indicators of the structural ordering in the films. From these measurements, we infer the degree of ordering in the films to be more than 85%.[25] Figure 1(b) shows the $\theta - 2\theta$ scan about (004) peak for films of various thickness on MgO and STO substrates. A clear shift of the Bragg reflections towards higher (lower) scattering angle (2θ) is seen for the films grown on MgO (STO) as the thickness is reduced. The out-of-plane lattice parameter (c) obtained from these scans decreases (increases) for the films grown on STO (MgO) with the increasing t. This can be understood in terms of the strain induced in the films due to lattice misfit. The positive misfit value for STO ($\epsilon = 2.4\%$) results in in-plane compressive strains, which decreases the in-plane lattice parameter (a) as verified by off-axis $\theta - 2\theta$ scans about (022) peak. Assuming the volume (a^2c) preserving distortion, we expect an increase in c with decreasing t for the films grown on STO. The films with lower thickness experience a relatively strong tetragonal distortion. As the film thickness increases, the distortion relaxes by formation of misfit dislocations and the in-plane strain $\epsilon_{xx}[= (a_{film} - a_{bulk})/a_{bulk}]$ approaches zero as seen in Fig. 1(c). We observe that the thinnest film ($t = 5$ nm) on STO is under highest biaxial compressive strain of $\epsilon_{xx} = \epsilon_{yy} = -0.44\%$ while the thicker films undergo partial strain relaxation with 100 nm film attaining bulk values. Similarly, the tensile strain in the Heusler alloy films on MgO disappears on increasing their thickness.

We now discuss the behavior of magnetic hysteresis loops [$M(H)$] for in-plane (along [110]) and out-of-plane (along [001]) field configurations [see Figs. 2(a)–2(c)]. The hysteresis loops of the film on MgO clearly show an in-plane easy axis for magnetization $(\vec{M})$ as revealed by the squareness of the loop in Fig. 2(a). This result is the same for thicker CFS films on STO [Fig. 2(b)]. However, for our thinnest film on STO, we observe a significantly higher

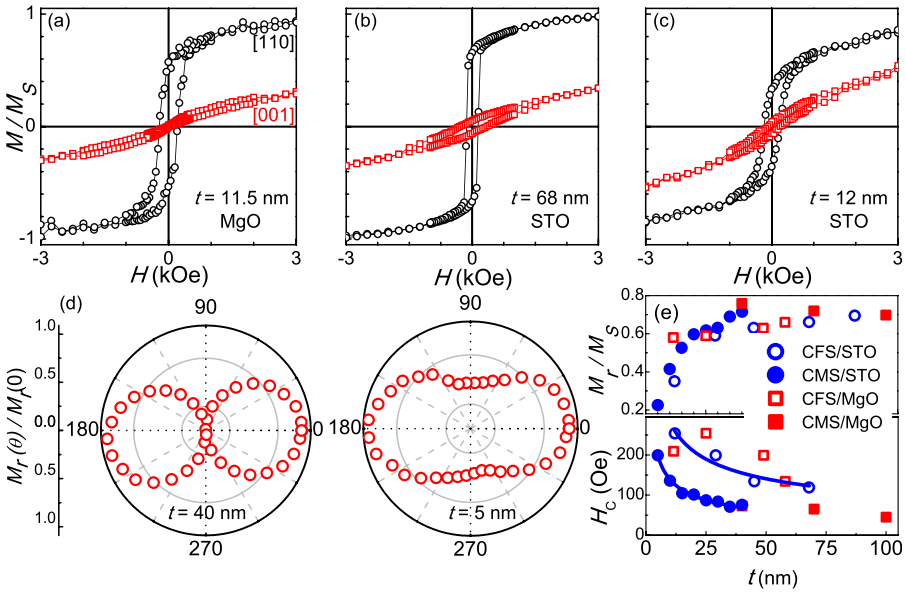

FIG. 2. The magnetic hysteresis loops measured along [110] and [001] directions at room temperature of (a) CFS (11.5 nm)/MgO as well as (b) 68 nm and (c) 12 nm thick CFS/STO films. (d) Polar plot of $M_r(\theta)/M_r(0)$ for 5 nm and 40 nm thick CMS/STO films at a step of 5°. Here $M_r(0)$ is the M_r at $\theta = 0°$. (e) The upper panel shows the thickness dependence of M_r/M_S, where M_S is the saturation moment. The Slater-Pauling formula predicts a M_S of $5\mu_B$ and $6\mu_B$ for CMS and CFS films, respectively.[26] We have used the experimental values of M_S, which are in reasonable agreement with the theory.[15] The lower panel shows the H_C as a function of t along with the fits (solid lines) according to the relation: $H_C \propto t^{-n}$.

out-of-plane magnetization, which suggests the possibility of tilted $\vec{M}$ with respect to the film plane. Figure 2(d) shows the remanent magnetization (M_r) at different angles (θ) of the field with respect to the film plane, which looks like a dumbbell with two lobes almost separated from each other for CMS(40 nm)/STO film. Clearly, the $M_r(\theta)/M_r(0)$ is maximum for $\theta = 0^\circ$ and 180° (in-plane directions) while it is almost zero at 90° and 270° (out-of-plane directions). This observation confirms the presence of in-plane easy axis for thicker films on STO. However, in the case of CMS(5 nm)/STO film, two lobes are joined, and thus the M_r is substantially higher for $\theta = 90^\circ$ and 270°. This suggests a canted easy axis instead of an in-plane one as observed in thicker films. We believe that the substrate-film interface plays an important role in tilting the magnetization away from the film plane. The upper panel in Fig. 2(e) shows the thickness dependence of the squareness (M_r/M_S) of magnetization extracted from in-plane $M(H)$ loops. In case of films on MgO, it remains almost constant whereas, for the films on STO, we notice a gradual decline in M_r/M_S with decreasing thickness, which indicates the deviation of easy axis from the film plane. Although the lowest observed value ($\approx$0.2 for 5 nm film) does not point towards a distinct out-of-plane easy axis, it certainly indicates some canting of $\vec{M}$ away from the film plane.

The coercivity of a material is the principal property related to the rate of change of magnetic relaxation between the remanent and demagnetized states. At absolute zero, it measures the barrier height that is required by magnetic moments to overcome the demagnetized state. The variation of the coercivity (H_C) of the films with thickness is plotted in the lower panel of Fig. 2(e). We observe that H_C decreases gradually with increasing thickness in all cases. This may be attributed to a lowering of defect concentration due to enhancing crystalline quality or due to lowering of strain in thicker films. Moreover, the reduction of H_C can also be due to the changes in the grain size and the surface roughness of the film with its thickness or related to the fact that the film thickness decreases to a point where the domain wall thickness becomes comparable to the film thickness. The H_C follows a power law type dependence on t of the form: $H_C \propto t^{-n}$ with $n = 0.50 \pm 0.02$ and 0.41 ± 0.17 for CMS and CFS films on STO, respectively. The value of n depends on the deposition conditions and the choice of ferromagnet and can have values from 0.3 to 1.5.[27–29]

We have carried out an analysis of the hard axis magnetization loops in the framework of Stoner-Wohlfarth formalism.[30] The total magnetic free energy (E) of the film in tetragonal symmetry can be expressed as

$$E = K_1 m_z^2 + K_2 m_z^4 + K_3 m_x^2 m_y^2 - \vec{M} \cdot \vec{H} + 2\pi M_s^2 m_z^2, \quad (1)$$

where K_1 and K_2 are second and fourth order uniaxial anisotropy constants, respectively, while K_3 is in-plane biaxial anisotropy constant. The $m_{x,y,z}$ are the direction cosines of the magnetization vector $\vec{M}$. The fourth term of Eq. (1) is the Zeeman energy and the last term represents the thin film demagnetization energy. For out-of-plane field hysteresis loop, i.e., when $\vec{H}$ is applied along [001], $\vec{M}$ will rotate from the [110] (in-plane easy axis) to [001] direction and thus the term $K_3 m_x^2 m_y^2$ is always zero. The minimization of total magnetic free energy for an out-of-plane field yields the equilibrium magnetization M in the field direction given by the relation

$$H = \left[\frac{2K_1}{M_S^2} + 4\pi\right] M + \frac{4K_2}{M_S^4} M^3. \quad (2)$$

The values of K_1 and K_2 can be obtained by fitting Eq. (2) to the hysteresis loops. The inset of Fig. 3(a) shows the plot of H/M vs M^2 for 68 nm thick CFS/STO film. The intercept and slope of the linear fit yield K_1 and K_2, respectively. The deviation in upper part of the curve from the linearity occurs as M approaches saturation, while the deviation at lower M can be attributed to magnetic domain effects.[31] All the films on MgO show in-plane easy axis without any substantial change in $M(H)$ loops with thickness. So the determination of anisotropy coefficients for these films will not be reliable while we observed clear change in $M(H)$ loops for the films on STO with varying thickness. Hence we will only focus on the later films in order to gain further insight of the magnetic state.

Figure 3 shows the values of K_1 and K_2 deduced from Eq. (2) for CF(M)S/STO films as a function of ϵ_{xx}. We clearly observe a monotonic increase in anisotropies with the increasing strain. Moreover, the values of K_1 are quite similar to previously reported values.[6] The K_1 is connected to ϵ_{xx} through the magnetoelastic coupling parameters and can be expressed

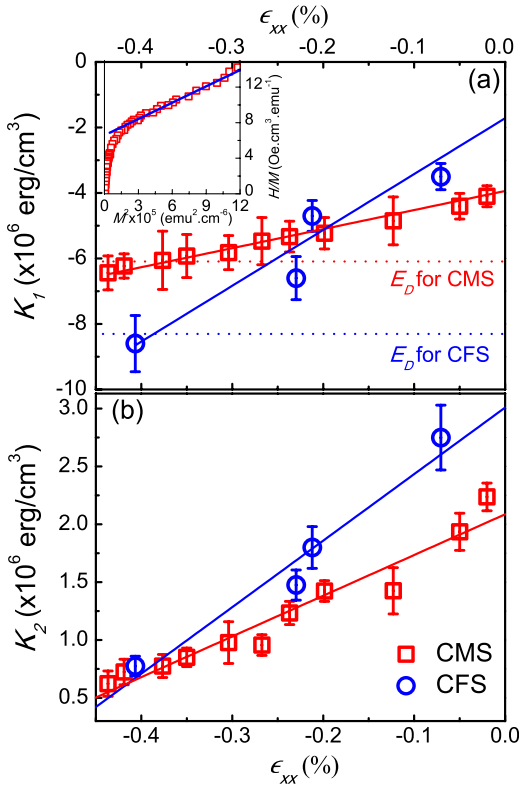

FIG. 3. (a) The second order uniaxial anisotropy constant (K_1) as a function strain (ϵ_{xx}) with the linear fits (solid lines). The ϵ_{xx} has been calculated using the values of a mentioned in Fig. 1(c). The dotted lines show demagnetization energy (E_D) for CF(M)S. The inset shows the plot of H/M vs M^2 for CFS (68 nm)/STO film along with the linear fit (solid line) given by Eq. (2). (b) The fourth order uniaxial anisotropy constant (K_2) as a function of ϵ_{xx} with the linear fits (solid lines).

as $K_1 = K_{mc} + 3\lambda\sigma_{xx}/2$.[32] The first term represents the strain independent magnetic anisotropy, commonly known as "magnetocrystalline anisotropy," which originates from the inherent crystal structure of ferromagnet.[32] The linear fits to $K_1(\epsilon_{xx})$ data yield $K_{mc} \approx -1.72 \times 10^6 \text{erg/cm}^3$ and $-3.94 \times 10^6 \text{erg/cm}^3$ for CFS and CMS, respectively [see Fig. 3(a)]. The second term is purely related to the strain induced anisotropy, which depends linearly on stress and the magnetostriction constant λ. The stress can be represented as $\sigma_{xx} = Y\epsilon_{xx}$, where the Young's modulus (Y) can be expressed in terms of elastic stiffness constants (C_{11} and C_{12}) as follows: $Y = (C_{11} - C_{12})(C_{11} + 2C_{12})/(C_{11} + C_{12})$.[33] Assuming theoretical values of C's,[34] we find $Y \approx 93$ GPa for CFS and 192 GPa for CMS. Using these values, the linear fits to $K_1(\epsilon_{xx})$ data yield $\lambda \approx (12.22 \pm 0.07) \times 10^{-6}$ and $(2.02 \pm 0.06) \times 10^{-6}$ for CFS and CMS, respectively. We are unaware of any values of λ and K_{mc} for these compounds reported in literature. The values of λ are comparable to the reported value of $\sim 15 \times 10^{-6}$ for another Heusler alloy Co_2MnAl (Ref. 35) while λ is of the order of 10^{-5} for half metallic manganites.[36,37] Our expression for K_1 in case of biaxial stress ($\sigma_{xx} = \sigma_{yy}, \sigma_{zz} = 0$) is same as the expression for uniaxial stress ($\sigma_{xx} \neq 0$, $\sigma_{yy} = \sigma_{zz} = 0$) induced anisotropy, i.e., $K = 3\lambda\sigma_{xx}/2$. However, these two cases are fundamentally different. In the former scenario, a uniaxial anisotropy is induced perpendicular to the plane (along z-axis) while, for the latter case, the uniaxial anisotropy is along the direction of applied stress (along x-axis). The other anisotropy constant K_2 also shows a linear dependence with ϵ_{xx} as shown in Fig. 3(b). Such linear relation has been predicted for a cubic system under biaxial strain and experimentally verified for Cu-Ni systems.[38] Similar to the case for K_1, we observe a substantial contribution to K_2 coming from magnetocrystalline origin in addition to the magnetoelastic couplings.

The direction of magnetic easy axis depends sensitively on anisotropy energies (K_1 and K_2) and the demagnetization energy $E_D (= 2\pi M_s^2)$. Only consideration of second-order term gives an out-of-plane magnetization state for $K_1/E_D < -1$ while $\vec{M}$ becomes in-plane for $-1 < K_1/E_D$. However, the fourth order anisotropy term introduces the canting states of $\vec{M}$ allowing a gradual transition between the in-plane and out-of-plane states.[23,38] Figure 4 shows the general single-domain magnetic phase diagram for a system with free energy given by Eq. (1) in zero magnetic field assuming a coherent rotation of magnetization. The films whose anisotropy data lie in region II have canted magnetization states, where the canting angle θ_c (the angle between $\vec{M}$ and film plane) can be obtained from the relation[37]: $\sin^2\theta_c = -(K_1 + E_D)/2K_2$. The CFS (12 nm)/STO film has $\theta_c = 41.5^\circ$ while the angles for 5 nm and 10 nm thick CMS/STO films are 31.8° and 17.9°, respectively. The data for thicker films fall into region I, which suggests that easy axis of magnetization is in-plane. Clearly, it can be inferred that easy axis changes from in-plane to canted orientation with increasing compressive strain. Hence, there is a possibility to get the perpendicular magnetic anisotropy in case of films with higher strain. This can be achieved either by lowering the film thickness or choosing a substrate with a larger positive misfit.

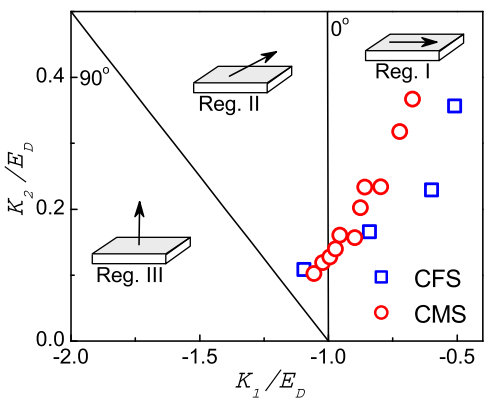

FIG. 4. The single-domain magnetic phase diagram demonstrating different stable magnetic states, namely, in-plane (region I), canted (region II) and out-of-plane (region III) state of magnetization. The symbols are the experimental data.

We have presented a study to correlate the crystallographic structure and the magnetic state of Co_2FeSi and Co_2MnSi films on (001) STO and MgO substrates. The films on STO are under in-plane biaxial compressive strain while a tensile strain is observed in the films on MgO. The strain gradually relaxes with increasing film thickness. The hysteresis loops clearly show an in-plane easy axis for all the films on MgO; however, for the films on STO, the out-of-plane component of magnetization increases with decreasing thickness. The analysis of magnetic free energy functional within the Stoner-Wohlfarth coherent rotation model with out-of-plane uniaxial anisotropy predicts a canted magnetization state for the films on STO, which gradually moves towards in-plane state with increasing thickness in a single-domain magnetic phase space. The uniaxial anisotropy terms have two distinct contributions; first one is intrinsic magnetocrystalline anisotropy, which is strain independent, and the other one is magnetoelastic anisotropy. We have extracted various anisotropy terms ($\sim 10^6 \text{erg/cm}^3$) and magnetostriction constants $\sim 10^{-6}$ for Co_2FeSi and Co_2MnSi. We also predict maximum canting angles of 41.5° and 31.8° for Co_2FeSi (12 nm) and Co_2MnSi (5 nm) on STO, respectively. These results prove that the epitaxial strain is a useful parameter to tailor the magnetic anisotropy in thin films of Heusler alloys, which could lead to the realization of out-of-plane magnetic anisotropy on oxide substrates for fabrication of memory devices.

The authors thank M. Shivakumar for his help in magnetization measurements. H.P. and P.K.R. acknowledge financial support from Indian Institute of Technology Kanpur and Council for Scientific and Industrial Research (CSIR), Government of India. This work is partly supported by CSIR, New Delhi [Grant No. 80(0080)/12/EMR-II]. R.C.B. acknowledges J. C. Bose Fellowship of the Department of Science and Technology, Government of India.

[1]M. I. Katsnelson, V. Yu. Irkhin, L. Chioncel, A. I. Lichtenstein, and R. A. de Groot, Rev. Mod. Phys. **80**, 315 (2008).
[2]T. Graf, C. Felser, and S. S. P. Parkin, Prog. Solid State Chem. **39**, 1 (2011).
[3]F. Y. Yang, C. H. Shang, C. L. Chien, T. Ambrose, J. J. Krebs, G. A. Prinz, V. I. Nikitenko, V. S. Gornakov, A. J. Shapiro, and R. D. Shull, Phys. Rev. B **65**, 174410 (2002).

[4]M. Belmeguenai, F. Zighem, Y. Roussigné, S.-M. Chérif, P. Moch, K. Westerholt, G. Woltersdorf, and G. Bayreuther, Phys. Rev. B **79**, 024419 (2009).
[5]W. H. Wang, M. Przybylski, W. Kuch, L. I. Chelaru, J. Wang, Y. F. Lu, J. Barthel, H. L. Meyerheim, and J. Kirschner, Phys. Rev. B **71**, 144416 (2005).
[6]H. Pandey, P. C. Joshi, R. P. Pant, R. Prasad, S. Auluck, and R. C. Budhani, J. Appl. Phys. **111**, 023912 (2012).
[7]H. Pandey and R. C. Budhani, J. Appl. Phys. **113**, 203918 (2013).
[8]S. Bosu, Y. Sakuraba, K. Uchida, K. Saito, T. Ota, E. Saitoh, and K. Takanashi, Phys. Rev. B **83**, 224401 (2011).
[9]L. J. Singh, Z. H. Barber, Y. Miyoshi, Y. Bugoslavsky, W. R. Branford, and L. F. Cohen, Appl. Phys. Lett. **84**, 2367 (2004).
[10]S. Trudel, G. Wolf, J. Hamrle, B. Hillebrands, P. Klaer, M. Kallmayer, H.-J. Elmers, H. Sukegawa, W. Wang, and K. Inomata, Phys. Rev. B **83**, 104412 (2011).
[11]M. Hashimoto, J. Herfort, H.-P. Scöhnherr, and K. H. Ploog, Appl. Phys. Lett. **87**, 102506 (2005).
[12]B. Jenichen, J. Herfort, T. Hentschel, A. Nikulin, X. Kong, A. Trampert, and I. Žižak, Phys. Rev. B **86**, 075319 (2012).
[13]H. Schneider, G. Jakob, M. Kallmayer, H. J. Elmers, M. Cinchetti, B. Balke, S. Wurmehl, C. Felser, M. Aeschlimann, and H. Adrian, Phys. Rev. B **74**, 174426 (2006).
[14]Anupam, P. C. Joshi, P. K. Rout, Z. Hossain, and R. C. Budhani, J. Phys. D: Appl. Phys. **43**, 255002 (2010).
[15]P. K. Rout, H. Pandey, L. Wu, Anupam, P. C. Joshi, Z. Hossain, Y. Zhu, and R. C. Budhani, Phys. Rev. B **89**, 020401(R) (2014).
[16]V. Toutam, H. Pandey, S. Singh, and R. C. Budhani, AIP Adv. **3**, 022124 (2013).
[17]M. S. Gabor, T. Petrisor, Jr., C. Tiusan, M. Hehn, and T. Petrisor, Phys. Rev. B **84**, 134413 (2011).
[18]Y. Liu, L. R. Shelford, V. V. Kruglyak, R. J. Hicken, Y. Sakuraba, M. Oogane, Y. Ando, and T. Miyazaki, J. Appl. Phys. **101**, 09C106 (2007).
[19]Z. Wen, H. Sukegawa, S. Mitani, and K. Inomata, Appl. Phys. Lett. **98**, 242507 (2011).
[20]R. F. Soohoo, *Magnetic Thin Films* (Harper & Row, New York, 1965).
[21]S. Kim, H. Lee, T. Yoo, S. Lee, S. Lee, X. Liu, and J. K. Furdyna, J. Appl. Phys. **107**, 103911 (2010).
[22]C. Du, R. Adur, H. Wang, A. J. Hauser, F. Yang, and P. C. Hammel, Phys. Rev. Lett. **110**, 147204 (2013).
[23]G. Singh, P. K. Rout, R. Porwal, and R. C. Budhani, Appl. Phys. Lett. **101**, 022411 (2012).
[24]X. W. Wu, M. S. Rzchowski, H. S. Wang, and Q. Li, Phys. Rev. B **61**, 501 (2000).
[25]Y. Takamura, R. Nakane, and S. Sugahara, J. Appl. Phys. **105**, 07B109 (2009).
[26]I. Galanakis, P. H. Dederichs, and N. Papanikolaou, Phys. Rev. B **66**, 174429 (2002).
[27]L. Néel, J. Phys. Radium **17**, 250 (1956).
[28]C. H. Tolman, J. Appl. Phys. **38**, 4538 (1967).
[29]I. W. Wolf, J. Appl. Phys. **33**, 1152 (1962).
[30]E. C. Stoner and E. P. Wohlfarth, Philos. Trans. R. Soc. London, Ser. A **240**, 599 (1948).
[31]Z.-H. Wang, H. Kronmüller, O. I. Lebedev, G. M. Gross, F. S. Razavi, H.-U. Habermeier, and B. G. Shen, Phys. Rev. B **65**, 054411 (2002).
[32]B. D. Cullity, *Introduction to Magnetic Materials* (Addison-Wesley, Reading, MA, 1972).
[33]H. M. Ledbetter and R. P. Reed, J. Phys. Chem. Ref. Data **2**, 531 (1973).
[34]X.-Q. Chen, R. Podloucky, and P. Rogl, J. Appl. Phys. **100**, 113901 (2006).
[35]J. J. Qiu, G. C. Han, W. K. Yeo, P. Luo, Z. B. Guo, and T. Osipowicz, J. Appl. Phys. **103**, 07A903 (2008).
[36]J. O'Donnell, M. S. Rzchowski, J. N. Eckstein, and I. Bozovic, Appl. Phys. Lett. **72**, 1775 (1998).
[37]S. E. Lofland, S. M. Bhagat, H. L. Ju, G. C. Xiong, T. Venkatesan, R. L. Greene, and S. Tyagi, J. Appl. Phys. **79**, 5166 (1996).
[38]K. Ha and R. C. O'Handley, J. Appl. Phys. **87**, 5944 (2000).